IEEE Photonics Technology Letters (2014), 26 (2), 198-201.
DOI: http://dx.doi.org/10.1109/LPT.2013.2291863

Modeling of Unwrapped Phase Defects in Modal Liquid Crystal Cylindrical Microlenses

Virginia Urruchi del Pozo, José Francisco Algorri Genaro, Juan Carlos Torres Zafra, and José Manuel Sánchez-Pena, *Senior Member, IEEE*[*]

***Abstract*—Liquid crystal (LC) lenses have been the subject of research due to their advantage of focal length tunability that brings added value to applications typically based on conven-tional gradient index lenses. A novel approach for modeling the unwrapped phase defects in modal LC microlenses is presented. For solving the gradual voltage across the lenses, the proposed analytical method uses only circuit theory exploiting partial differential equations and conformal mapping techniques. The LC molecular ordering has been modeled on the basis of the continuum theory and optical response has been deduced through inspection of phase retardations. The model validity has been checked for predicting some defects of the modal microlenses in the phase of the lens design, comparing experimental character-ization with simulation.**

***Index Terms*—Conformal mapping, liquid crystals, lenses, partial differential equations (PDEs).**

I. Introduction

LIQUID crystal (LC) lenses have been subject of research for over 30 years. During that time, there have been constant improvements, since LC provides advantages like weight and volume reduction and mainly focal length tunability. Some research works have been reported to promote this feature, such as focusing a light beam on a spot [1], beam steering control in curved trajectories of light [2] or imaging in optical systems [3]. By reducing the size of lenses to a micrometric scale with one (linear) or two-dimensional (2-D) array structures, the range of applications can be extended further. For example, one-dimensional cylindrical lenses have been proposed for 3D imaging [4] and 2-D lens arrays proven for read-out DVD information [5]. Particularly, the implementation of cylindrical lenses is a highly topical issue for generating 3D imaging in autostereoscopic systems [6]. LC lenses acts as GRadient INdex (GRIN) lenses which show a continuous change of the refractive index within the structure. Modal control is a technique that consists of generating a radial graded refractive index across the lens aperture by using a layer of high sheet resistance (MΩ/sq) as a control electrode. The thickness and composition of the control layer are key parameters for the design. A theoretical model of its operating principle means an effective tool oriented to predict the electrooptic response before fabrication. There has been reported in the literature a model that describes the effective voltage distribution on the control electrode for modal lenses by a capacitive – resistive voltage divider in the aperture area [7] that is only valid at the millimeter scale. It considers just a single resistive electric effect for the layer of high sheet resistance. Despite this model has been widely applied for some research groups [8], [9], the model reported is limited to lenticular devices with the aperture/thickness ratio higher than 2-3 [10]. In addition, it does not include distributed capacitances whose effect is negligible if not considered micrometric scale devices. As the lens sizes approaches the micrometer scale, the modal control layer becomes unnecessary. Then, the fringe field effect turns significant and the capacitive effects in the coplanar electrode structure of the resultant hole-patterned scheme must be taking into account. Depending on the transition between both schemes, the horizontal electrical impedance can be predominantly capacitive, resistive or a combination of both.

In this letter, the equivalent electrical circuit (EEC) including both the capacitive and resistive effects has been applied for the first time, to the best of our knowledge, for modeling some unwrapped phase defects in modal LC cylindrical microlenses. It has been reported that this EEC models appropriately the electrooptic response of some LC lenses based on modal and hole-patterned electrode schemes without defects. The main shortcoming modeled in this letter is a shrinking effect of the aperture that appears as a result of an unsuitable design. A computer application to simulate the molecular position, and the electric and optic behavior of these devices, has been programmed. It requires some input parameters: LC constants (elastic and dielectric), fabrication parameters (resistivity of the control electrode, thickness, etc.) and driving signals. For solving gradual voltage across the lenses, proposed method uses only circuit theory applied to the EEC, becoming a non complex task. Simulation results of the unwrapped phase defects have been compared with experimental characterization of modal lens arrays filled with high birefringence nematic LC.

II. Simulation of LC Microlens Electrooptic Response

The structure and dimensions of LC lenses considered in this letter are focused on an application for a lenticular array in an autostereoscopic system. The suggested scheme is a cylindrical array configuration [11]. Lenses of the array

*This work was supported in part by the Ministerio de Ciencia e Innovación of Spain under Grant TEC2009-13991-C02-01 and in part by the Comunidad de Madrid under Grant FACTOTEM2 S2009/ESP-1781.

Fig. 1. Left: 3D view of the proposed scheme for a cylindrical LC lens. Right: Electrode pattern for the lens top plate. Note that, taking the right drawing as a reference, plates are located parallel to the paper plane. Sizes are not to scale.

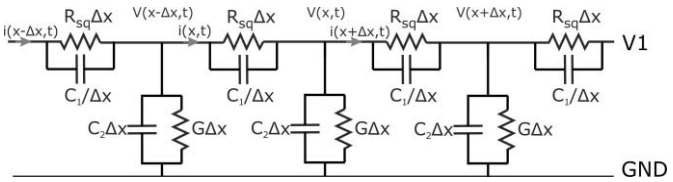

Fig. 2. Advanced equivalent electric circuit (EEC) based on a transmission line for modeling modal liquid crystal microlenses.

reproduce a parabolic refraction index gradient in the LC layer, so mimicking the optical behavior of conventional lenses. The electrode patterns consist of two comb interdigitated electrodes (Fig. 1). One of the comb electrodes was fabricated as a third electrode for measurement purposes in the center of each lens. The proposed method for simulation of lenses' electrooptic response can be summarized basically in three steps: the EEC modeling, the molecular order modeling and the optical response deduction.

Firstly, the gradual voltage has been modeled by considering the complete equivalent electric circuit (EEC) consisting of a transmission line with coplanar capacitances (Fig. 2). The key electric components that explain the modal behavior are the distributed resistances (R_{sq}) across the surface of the lens pitch [12] that model the typical high resistivity electrode for modal lenses. In this arrangement, the capacitances (C_1) describe the parasitic capacitances between teeth of the comb electrode for the LC microlens. Distributed capacitances and resistances are connected in parallel in the transmission line circuit. The rest of the components are: C_2 and G, that is, capacitance and conductance of the LC layer. Δx represents the length increment. An analytical method has been employed to derive the spatially non-uniform electric field on the transmission line. This approach, based on *Partial Differential Equations* (PDE), is introduced for the first time in these structures to deduce V(x), voltage V in the LC surface depending on x, the position at the lens aperture from its center. Considering a driving voltage that comprises only one harmonic, $V(x,t) = V(x) \cdot e^{j\cdot\omega\cdot t}$, simplified PDE satisfied by voltage can be expressed as,

$$\frac{\partial V^2(x)}{\partial x^2} = \frac{G + j\omega C_2}{\frac{1}{R_{sq}} + j\omega C_1} \cdot V(x) = \Psi \cdot V(x) \qquad (1)$$

where ω is the angular frequency and Ψ represents the frequency dependent term. PDE of (1) has been solved with MATLAB software. The main advantage of this approach relies on the potential of defining the voltage at each position x, across the lens aperture, the ratio with the maximum voltage and a critical design parameter, the resistivity of the control electrode. Distributed capacitance C_1 has been evaluated following *conformal mapping* techniques [13]. Those techniques have a wide scope of application in the field of capacitance modeling, particularly for capacitances between coplanar electrodes in MOSFET transistors, microstrip lines, etc. In this letter, a simple expression for the capacitance between tracks, C_1, obtained by this method, is given by

$$C_1 = \varepsilon_0 \cdot \varepsilon_1 \cdot \frac{d}{A}(F) \qquad (2)$$

that is, as a function of vacuum permittivity, ε_0, the LC permittivity in the parallel direction to the glasses, ε_1, the LC thickness, d, and the parameter A. This parameter has been estimated by using conformal mapping techniques based on the Christoffel–Schwarz transformation [14],

$$A = \frac{2K(k)}{K(k')} \text{ with } k = \frac{W_1}{W_1 + 2W_2},\ k' = \sqrt{1-k^2} \qquad (3)$$

where W_1 is the space between electrodes (the cylindrical lens diameter), W_2 the electrode width, K(k) the complete elliptic integral of the first kind and k the elliptic modulus.

On the other hand, the LC molecular ordering inside the device has been modeled on the basis of the continuum theory. This approach includes the effect of the energy arising from the electric field distribution across the lens aperture. In nematics, the elasticity is associated with the spatial variation of the director $\vec{n}$. A gradient of $\vec{n}$ gives rise to an elastic energy and a restoring force associated. This energy, F_d, is defined by the Frank-Oseen's free energy equation (4). It is mathematically described in terms of the three elastic modes associated to the three Frank elastic constants of a uniaxial nematic LC (K_{ii}) and their characteristic deformations. Besides, if an static electric field, E, is applied to the nematic LC sample, free energy related to the interaction between the field and the LC, F_e, is in equation (5),

$$F_d = \frac{1}{2}\left\{ K_{11}\left(\nabla\cdot\vec{n}\right)^2 + K_{22}\left(\vec{n}\cdot\nabla\times\vec{n}\right)^2 + K_{33}\left|\vec{n}\times\nabla\times\vec{n}\right|^2\right\} \qquad (4)$$

$$F_e = -\frac{1}{2}\varepsilon_0\left(\Delta\varepsilon\left(\vec{n}\cdot\vec{E}\right)^2 + \varepsilon_\perp\cdot\vec{E}\cdot\vec{E}\right) \qquad (5)$$

where ε_0 is the vacuum permittivity, $\Delta\varepsilon$ the LC relative dielectric anisotropy and $\varepsilon_\perp$ the perpendicular permittivity. To obtain the equilibrium configuration for the director and the solution of its orientation, the total free energy, or Gibbs free energy, $F_G = F_d + F_e$, must be minimized. For solving the minimization of the non-linear, second order, boundary value problem, the Bvp4c numerical method (integrated in MATLAB software), has been employed since error is minimized. In addition, the electrical simulations can be performed with high electrical voltages.

Finally, by knowing angular LC ordering, the effective refractive index (n_{eff}) is obtained. It depends also on LC ordinary and extraordinary refractive indices, n_o and n_e, respectively. Then, the average refractive indices and the phase retardations are mathematically obtained at each position x. The developed program graphically depicts LC molecular distribution inside the cell in 2D images of transversal sections of the sandwich from the top to the bottom electrodes. Also,

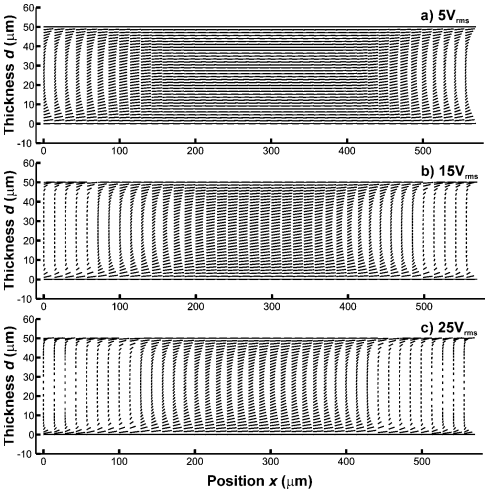

Fig. 3. Simulation of molecular arrangement for some representative values of voltage: (a) 5 V_{rms}, (b) 15 V_{rms} and (c) 25 V_{rms}. Electrodes of the glass plates are vertical, perpendicular to the paper plane, in positions 0 and 570 μm. Glass plates are horizontal, in positions 0 and 50 μm.

voltage gradient electrically induced and phase profiles are graphed. The unwrapped phase defects of the LC cylindrical microlenses can be described and discussed from the diagrams.

III. Simulation Results and Discussion

Previous to the fabrication of the lenses, some simulations of the electrooptic response were carried out. The starting parameters were chosen for allowing us to predict some specific electrooptic responses, so that the performance of the developed program was proven.

The parameters of the LC mixture considered for simulations (nematic MDA-98-1602 from Merck) were $n_e = 1.7779$, $n_o = 1.5113$ ($\Delta n = 0.2666$ at 589nm) and $\varepsilon_e = 16.2$, $\varepsilon_o = 4.3$ ($\Delta\varepsilon = 12$, 1kHz). The elastic constants were $K_{11} = 13.6$ pN, $K_{22} = 15.7$ pN, K_{33} / $K_{11} = 1.15$ and the rotational viscosity $\gamma_1 = 203$ mPa·s (20 °C). A suitable layer sheet resistance was 3 ± 0.3 GΩ/sq [15].

Assuming the microlens structure defined initially, devices were manufactured with 50 μm thickness and 570 μm diameter of each individual lens of the array. The electrooptic characterization of the devices was realized. The lens properties were observed by interference method using He–Ne laser beam (632.8 nm) as a light source. CCD images were captured automatically by a MATLAB image recognition program developed with this purpose in view. The specific manufacturing parameters of this array make this modal device independent of the capacitance C_1.

By inspection of Fig. 3, molecular ordering can be described. Those diagrams include the solution of the director orientation for some representative values of voltage, 5 V_{rms}, 15 V_{rms} and 25 V_{rms}, 1 kHz AC square signal. They represent 2D images of transversal sections of the sandwich from the top to the bottom electrodes. For 5 V_{rms} (Fig. 3 (a)), it is noticed that the voltage distribution drops below the threshold before reaching the center of the lens, since there are some molecules which position remains unswitched. It reveals a too large sheet resistance of the control electrode for this approach that can be foreseen in the phase of the lens design. On the other hand, a too long lens diameter forces high driving voltages for generating a phase gradient that spreads out over the lens surface. Such high voltages give rise to undesirable shrinking effect of the lens aperture, probably caused by saturation of the tilt angle of the molecules near the lens edges (Fig. 3 (b), 25 V_{rms}). Besides, the shrinking effect resulted in a significant decrease of the aperture diameter of the lenses.

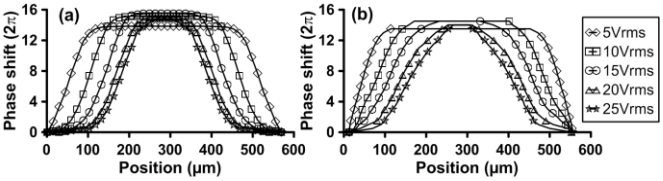

Fig. 4. Phase shift profiles of a cylindrical LC lens as a function of control voltage. (a) Simulation results. (b) Measurements of characterization.

Figs. 4(a) and 4(b) graph some simulations and measurements, respectively, of the unwrapped phase defects in the modal LC cylindrical microlens, both as a function of the driving voltage amplitude (rms). A set of only five voltage values has been chosen for clarity of the plot. The simulation of the unwrapped phase means a mathematical translation of the molecular arrangement to optical behavior. Thus, reasoning about the phase, for the smallest voltages the behavior involves the growing of a flat-like phase in the center of the lens, that is, without any change in the phase retardation. This fault is shown in Figs. 4(a) and 4(b), for 5 V_{rms}. Next, the flat-like phase is erasing in the voltage transition from 10 V_{rms} to 15 V_{rms}. But a decrease of the lens aperture arises, as stated with the description of the molecular orientation, for those values. The worst performance is obtained for the saturation voltage, 25 V_{rms} and a shrinking effect is illustrated again with this measure. Both simulated and experimental unwrapped phase profiles are not parabolic due to a non-optimal design. This drawback could be prevented mainly caring for the design of the dimensions of the device.

Some viewpoints are argued to discuss the disparities between the simulations and the measurements of the unwrapped phase defects. Firstly, the results are subject to the experimental set-up. So, there are reasonable deviations of the current phase magnitude that can be attributed to the temperature and laser power fluctuations. The experiments have been carried out at room temperature while the LC datasheet parameters are specified to 20 °C. The wavelength dependence of the results is not relevant since the birefringence from the datasheet, $\Delta n = 0.2666$ at 589nm, and the one measured for 632.8nm, $\Delta n = 0.2642$ (and used in the simulation program), are very similar. Besides, some tolerances of the manufacturing parameters are regarded as hypothesis thus leading to delimit an optimal margin of the device operation. In this point, the simulation algorithm has considered some cell gap values that lie within the interval 50 ± 5 μm, and also a slight 10% manufacturing tolerance of the sheet resistance (3 ± 0.3 GΩ/sq). In addition, some phase disparities between simulations and measurements can come from the difficulty of convergence of the algorithm for this boundary value problem as high voltages (more than 6 V_{rms}) are applied to the device. The numerical methods usually cause instabilities

that have been solved by using specific MATLAB functions. Few examples in the literature have demonstrated the solution for high voltages [16].

From the experimental point of view, the results are strongly dependent on the width of the capture window for recording the interference patterns in the demodulation of the wrapped phase. The absolute phase magnitude and the threshold voltage are directly related to it. For this approach, a wide enough window has been used in practice. The discrepancies between the switching threshold voltages also owe to only the simulations contemplate the strength of the alignment layer anchoring [17] that forces a unchanged optical axis at a specific distance from the glass plates.

The discussion concludes that these results are indicative of the successful extension of the modeling of the unwrapped phase to defects in modal LC microlenses. The input program parameters are the key to design different kinds of microlenses without defects. The validation of the application has been probed and both results are fairly in agreement.

IV. Conclusion

A method based on the application of the circuit theory on an optimized equivalent electrical circuit has been proposed and applied for modeling some unwrapped phase defects in modal LC cylindrical microlenses. The equivalent circuit has a horizontal electrical impedance that includes both capacitive and resistive effects. The shrinking effect of the lens aperture can be modeled in the phase of the lens design. The proposed method is simpler and faster than other methods based on finite elements.

References

[1] S. P. Kotova, V. V. Patlan, and S. A. Samagin, "Tunable liquid-crystal focusing device. 2. Experiment," *Quantum Electron.*, vol. 41, no. 1, pp. 65–70, 2011.

[2] S. Davis, *et al.*, "Electro-optic steering of a laser beam," *SPIE Newsroom*, Jun. 2011, DOI: 10.1117/2.1201105.003715 [Online]. Available: http://spie.org/x48401.xml

[3] W.-C. Hung, Y.-J. Chen, C.-H. Lin, I.-M. Jiang, and T.-F. Hsu, "Sensitive voltage-dependent diffraction of a liquid crystal Fresnel lens," *Appl. Opt.*, vol. 48, no. 11, pp. 2094–2098, Apr. 2009.

[4] Y.-P. Huang, C.-W. Chen, T.-C. Shen, and J.-F. Huang, "Autostereoscopic 3D display with scanning multi-electrode driven liquid crystal (MeD-LC) lens," *3D Res.*, vol. 1, no. 1, pp. 39–42, 2010.

[5] M. Hain, R. Glöckner, S. Bhattacharya, D. Dias, S. Stankovic, and T. Tschudi, "Fast switching liquid crystal lenses for a dual focus digital versatile disc pickup," *Opt. Commun.*, vol. 188, nos. 5–6, pp. 291–299, 2001.

[6] H. Lee, G.-M. Um, and C. Kim, "A portable, seamless 3D display without glasses," *SPIE Newsroom*, Aug. 2011, DOI: 10.1117/2.1201108.003818 [Online]. Available: http://spie.org/x52121.xml

[7] S. P. Kotova, V. V. Patlan, and S. A. Samagin, "Tunable liquid-crystal focusing device. 1. Theory," *Quantum Electron.*, vol. 41, no. 1, pp. 58–64, 2011.

[8] N. Fraval and J. L. de Bougrenet de la Tocnaye, "Low aberrations symmetrical adaptive modal liquid crystal lens with short focal lengths," *Appl. Opt.*, vol. 49, no. 15, pp. 2778–2783, 2010.

[9] S. P. Kotova, *et al.*, "Modal liquid crystal wavefront corrector," *Opt. Express*, vol. 10, no. 22, pp. 1258–1272, 2002.

[10] S. Sato, "Applications of liquid crystals to variable-focusing lenses," *Opt. Rev.*, vol. 6, no. 6, pp. 471–485, 1999.

[11] V. Urruchi, J. F. Algorri, J. M. Sánchez-Pena, M. A. Geday, X. Quintana, and N. Bennis, "Lenticular arrays based on liquid crystals," *Opto-Electron. Rev.*, vol. 20, no. 3, pp. 260–266, 2012.

[12] A. F. Naumov, M. Y. Loktev, I. R. Guralnik, and G. Vdovin, "Liquid-crystal adaptive lenses with modal control," *Opt. Lett.*, vol. 23, no. 13, pp. 992–994, Jul. 1998.

[13] R. Igreja and C. J. Dias, "Analytical evaluation of the interdigital electrodes capacitance for a multi-layered structure," *Sens. Actuators A, Phys.*, vol. 112, nos. 2–3, pp. 291–301, 2004.

[14] S. S. Gevorgian, T. Martinsson, P. L. J. Linnér, and E. L. Kollberg, "CAD models for multilayered substrate interdigital capacitors," *IEEE Trans. Microw. Theory Tech.*, vol. 44, no. 6, pp. 896–904, Jun. 1996.

[15] V. Urruchi, J. F. Algorri, J. M. Sánchez-Pena, N. Bennis, M. A. Geday, and J. M. Otón, "Electrooptic characterization of tunable cylindrical liquid crystal lenses," *Molecular Cryst. Liquid Cryst.*, vol. 553, no. 1, pp. 211–219, 2012.

[16] Q. Wang, S. He, F. Yu, and N. Huang, "Iterative finite-difference method for calculating the distribution of a liquid-crystal director," *Opt. Eng.*, vol. 40, no. 11, pp. 2552–2557, 2001.

[17] C.-C. Wang, M.-J. Jang, and P.-L. Ko, "A measurement system for the phase retardation of liquid crystal particles under an electric field effect," *J. Phys., Conf. Ser.*, vol. 48, no. 1, pp. 957–969, 2006.